Poloidal polarimeter for current density measurements in ITER

A. J. H. Donné[a] and M. F. Graswinckel
FOM-Institute for Plasma Physics Rijnhuizen, Association EURATOM-FOM, PO Box 1207, 3430 BE Nieuwegein, The Netherlands[b]

M. Cavinato, L. Giudicotti, and E. Zilli
Consorzio RFX, Corso Stati Uniti 4, 35127 Padova, Italy

C. Gil
CEA Cadarache, 13108 Saint-Paul-lez-Durance, France

H. R. Koslowski
Institut für Plasmaphysik, Forschungszentrum Jülich GmbH, D-52425 Jülich, Germany

P. McCarthy, C. Nyhan, S. Prunty, and M. Spillane
University College Cork, Ireland

C. Walker
ITER International Team, Boltzmannstrasse 2, D-85748 Garching-bei-München, Germany

(Received 28 April 2004; accepted 25 July 2004; published 1 November 2004)

One of the systems envisaged for measuring the current density profile in the ITER is a 118 μm poloidal polarimeter system. The proposed system has two independent views: one fan of chords observes the plasma via an equatorial port and a second fan views down from an upper port. This article will present the status of the on-going work and will address issues as sensitivity and accuracy, refraction, Gaussian beam ray-tracing, alignment, and calibration as well as some specific design details. © *2004 American Institute of Physics.* [DOI: 10.1063/1.1804372]

I. INTRODUCTION

Control of the current density profile is essential for the so-called advanced modes of tokamak operation. The main techniques to measure this profile are based on the Faraday effect, experienced by a far-infrared beam passing through the plasma (called polarimetry)[1] and on the motional Stark effect (MSE)[2] experienced by energetic neutral beam atoms that are injected into the plasma. Both techniques have their specific advantages and, therefore, both of them are being explored for the ITER tokamak (ITER=Latin word for "The way"). This article will focus on the poloidal polarimeter system for ITER. In Sec. II the overall optical setup along with the results of (Gaussian beam) ray-tracing calculations including refraction will be presented. In Sec. III the values for the Faraday rotation angles and the ellipticity that can be expected are discussed for various ITER operational scenarios, along with the envisaged accuracy in the determination of the current density profile. In Sec. IV the characteristics of the retroreflectors to be employed are discussed. Gaussian-beam ray-tracing calculations of one of the polarimetry chords all the way from the retroreflector to the diagnostics laboratory have been performed to assess alignment issues and to study the optical tolerances. The results of these calculations are presented in Sec. V. The article will be concluded with an outlook including suggestions for further work.

[a]Author to whom correspondence should be addressed; electronic mail: donne@rijnh.nl
[b]Partners in the Trilateral Euregio Cluster.

II. BASIC GEOMETRY AND LAYOUT

The polarimeter under study is an evolution of the system that was originally proposed for ITER-98.[3] That system featured a fan of chords viewing the plasma through an equatorial port and was envisaged to operate at a wavelength of 118 μm. Because the geometry of ITER has changed with respect to that of ITER-98, the maximum number of chords via the equatorial port is now limited to 9 (see Fig. 1), viewing the plasma via two penetrations through the blanket modules. The change of geometry has happened in parallel to the work reported here. This explains why in some figures calculations for eight chords are shown. Since in all cases the calculations have been done for the same plasma geometry this does not have an effect on the conclusions of this article.

To optimize the coverage of the plasma also four chords via an upper plug are proposed. Additional chords looking up from the divertor have been used for a small part of the underlying study. The beams are reflected back along the same path through the plasma by means of 37 mm wide retroreflectors indented about 25 cm deep at the bottom of remote handling grips in the blanket modules opposing the ports. The chord geometry is essentially fixed by the fact that the retroreflectors can be only positioned at a number of discrete slots in the blanket modules and the additional desire to minimize the number and size of port penetrations to reduce as much as possible the neutron streaming through the port plugs. It may be obvious that, because of their proximity to the plasma, the retroreflectors are the most critical element in the setup.

In the design of the optical system the rule of thumb was

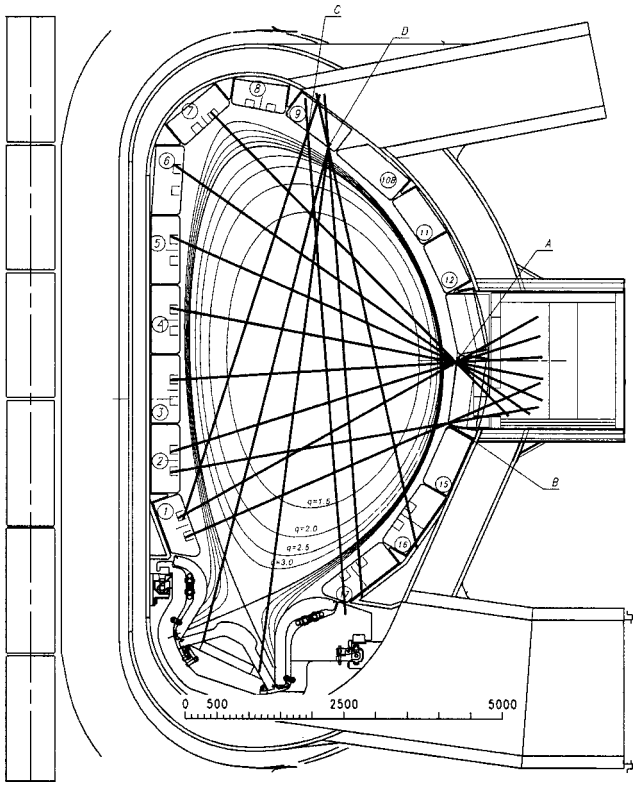

FIG. 1. Overview of the proposed polarimeter system for ITER.

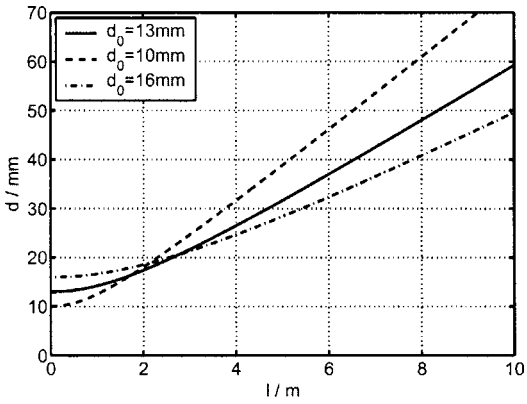

FIG. 2. Expansion of the beams for different beam waists at the position of the retroreflectors.

used that the dimensions D of apertures and mirror diameters should be larger than the limit $D_{\min} > 2.2d$, with d the $1/e$ width of the intensity distribution of the laser beam.[4] This corresponds to a 99.2% reflection/transmission by/through the optical component. Since the maximum possible diameter of the retroreflector is limited to 37 mm (i.e., the width of the remote handling grips in the blanket modules), this was used as a starting point for the gaussian beam ray-tracing calculations. To avoid vignetting by the retroreflector, the beam focus at the retroreflector should have a diameter smaller than 16.5 mm. In Fig. 2, the beam expansion is shown for three diameters of the beam waist: a larger beam waist leads to a smaller diameter of the beam in the port plug. To allow for some small beam misalignments on the retroreflectors a 13 mm diameter beam waist was used as design guideline. The distance between the retroreflector and the port penetration is in the range 4.5–5.5 m (depending on the chord) and that between the retroreflector and the second mirror (being the first focusing element seen from the plasma) is between 6.5 and 7.5 m. Applying again the rule of thumb, this implies that blanket penetrations with a diameter of 100 mm are sufficiently large for the lateral fan of viewing lines. This incorporates even some margin for slight misalignments of the beam and the use beam steering for alignment purposes. Apart from the second mirror only one other focusing mirror per chord is needed to guide the laser beam all the way from the retroreflectors to the diagnostics laboratory (see Table I, Fig. 3). All other reflective elements are plane mirrors.

In principle also a blanket penetration of 100 mm diameter would be large enough for the additional vertical viewing lines. However, to be able to correct for possible misalignments and the requirement for beam sweeping (see Sec. V) a somewhat larger diameter (120 mm) is preferable.

Albeit not very critical for the optical system, it is tempting to minimize the number of optical components in the setup. Nevertheless, the viewing penetrations should have a sufficiently high number of bends to reduce the neutron streaming and also to correct for differential movements of the various parts of the ITER device. Furthermore, a double vacuum barrier is needed. This will be made up of two

TABLE I. Coordinates of all optical elements in the beam line of polarimeter chord No. 5 (see Fig. 1).

Number	Element	X(mm)	Y(mm)	Z(mm)	Focal length (mm)	Cumulative distance (mm)
1	Retroreflector	−4048.70	−1937.62	1803.30		0.00
2	Plane mirror	−9057.60	−1937.62	284.50		5234.10
3	Spherical mirror	−9057.60	−1733.32	284.50	5100.00	5438.40
4	First window	−11 004.94	−1733.32	482.00		7395.73
5	Plane mirror	−12 598.62	−2014.33	482.00		9014.00
6	Second window	−12 598.62	−2014.33	818.00		9350.00
7	Plane mirror	−12 598.62	−2014.33	1154.00		9686.00
8	Plane mirror	−12 773.31	−1023.61	1154.00		10 692.00
9	Plane mirror	−17 640.86	−1881.89	1154.00		15 634.64
10	Plane mirror	−17 640.86	−1881.89	2862.50		17 343.14
11	Plane mirror	−17 403.25	−2695.49	2862.50		18 190.73
12	Spherical mirror	−33 250.00	−7323.44	2862.50	72 00.00	34 699.43

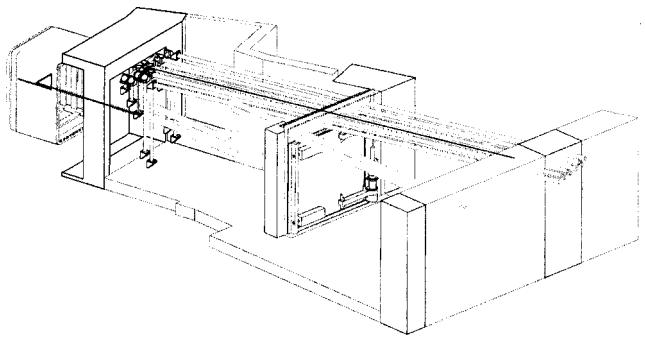

FIG. 3. Overview of the optical transmission line from the position of the first vacuum window (No. 4 in Table I) to the point of entrance into the diagnostic laboratory (No. 12).

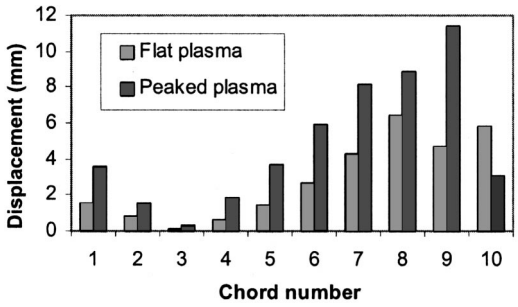

FIG. 4. Effect of refraction on the position of the beam on the retroreflectors (in a direction perpendicular to the chord). Chords 1–8 are for the equatorial port system, while chords 9 and 10 are two of the chords viewing via the upper port.

vacuum windows separated by a 90° mirror. The two windows each need to tilted by a small angle to avoid backreflections and to have a minimum distortion on the beam polarization.[3] If the amplitude of the backreflected signal arriving at the detector is even as small as 1%, this leads to an additional error in the measurement of the Faraday rotation angle of 0.1 deg.[5] The space between the two windows is separately pumped. An overview of the beam line from the first window to the entrance of the diagnostics laboratory is shown in Fig. 3. The coordinates of all optical elements are indicated in Table I.

Ray-tracing calculations have been done for ITER plasmas with two different density profiles: $n_e = 10^{19} + a \times 10^{20} \times (1-\rho^b)\mathrm{m}^{-3}$, with ρ the radial coordinate, being 0 in the plasma center and 1 at the edge. Both a flat (ITER reference) density profile with $a=1$ and $b=10$, and a peaked profile with $a=2$ and $b=2$ have been studied. The beam displacement due to refraction varies from chord to chord and is typically between 1 and 6 mm for the equatorial chords and the flat density profile (see Fig. 4). The refraction for the peaked profile and for the vertical chords, with a much longer line of sight through the plasma is somewhat larger (up to 12 mm in the worst case). It is important to note that the difference in the beam displacements calculated for the flat and for the peaked profile is typically between 1 and 1 mm (depending on the chord). These small displacements can be easily corrected by appropriate beam steering (see Sec. V). They also demonstrate that the system is relatively insensitive to changes in the shape of the density profile, albeit that one should carefully take this effect into account when dimensioning the mirrors. For instance a 4 mm misalignment of the beam on the retroreflector of chord No. 5, would lead to a misalignment of the beam on almost all components in the beam line (see Fig. 5). So either the optical components should have a large enough dimension to incorporate these misalignments, or one should make use of active beam steering (see Sec. V).

The effect of electron cyclotron absorption has not been separately studied for ITER. However, in the earlier study for ITER-98 it was already concluded that absorption by very high harmonics of the electron cyclotron frequency was completely negligible under all conditions.[3] Since the highest electron cyclotron emission frequencies expected in ITER are lower than those in ITER-98, this conclusion is still valid.

III. SENSITIVITY OF THE SYSTEM

The Faraday rotation angles and ellipticity have been calculated for a range of ITER equilibria during a nominal inductive scenario that is envisaged for ITER (see Table II). The vacuum toroidal field in all these cases was equal to 5.3 T. Furthermore, two other equilibria have been considered. One of them is a 17 MA plasma at the end of the burning plasma phase, and the other is the equilibrium corresponding to a reversed shear plasma with a plasma current of 10 MA. All equilibria have been calculated for six different density profiles (see Fig. 6).

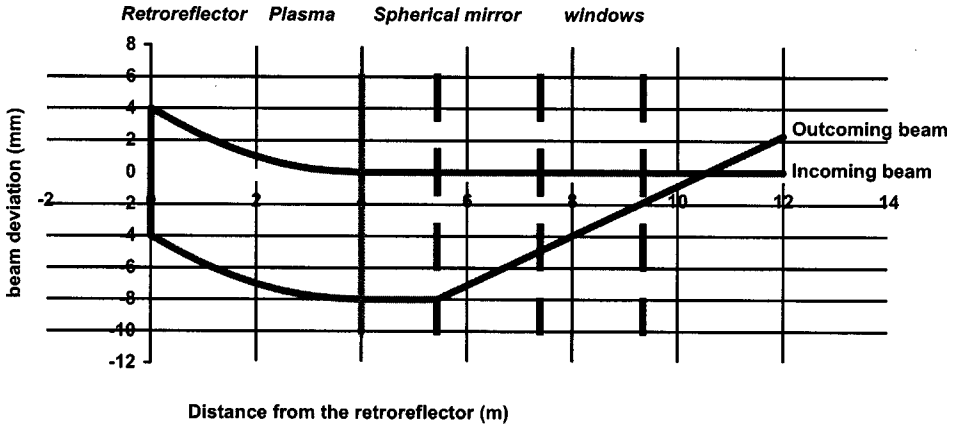

FIG. 5. Effect of the 4 mm beam displacement on the retroreflector of chord No. 5 on the full beam trajectory.

TABLE II. Plasma current I_p, central safety factor q_0, and plasma pressure p_{tot} for the series of equilibria during a normal inductive scenario.

I_p(MA)	q_0	*ptot* (0) (Mpa)	Remarks
5.5	2.14	0.03	
6.5	2.02	0.03	
7.5	1.79	0.04	*X*-point formation
8.5	1.61	0.05	
9.5	1.47	0.07	
10.5	1.36	0.08	
11.5	1.28	0.09	
12.5	1.18	0.11	
13.5	1.13	0.13	
15.0	1.05	0.16	Start of current flat-top
15.0	0.99	0.99	Start of burn
15.0	0.99	0.99	End of burn
12.2	0.83	0.14	End of cooling

The calculations of the Faraday rotation angle and the ellipticity (related to the Cotton–Mouton effect) were done by cutting the plasma in slabs of 1 cm thickness and calculating the transformation matrices of an electromagnetic wave traveling through this slab and by applying these matrices to the electric field vector of the beams. Refraction in the plasma due to density gradients was neglected in this part of the study. The calculations were done for single passage through the plasma only. So all values given below should be multiplied by 2. The MATLAB computer program for these calculations was originally developed by Nieswand.[6]

Here we will only present as example the calculations for a fan of beams through the equatorial port and for the flat density profile. The calculated values of the Faraday rotation angle and the ellipticity are rather large (see Fig. 7) and can be easily measured with high accuracy. Also the dependence of the slope of the Faraday rotation profile on the central safety factor is easily measurable with sufficient accuracy, even in the reversed shear case, where the rotation angles are typically a factor of 2 smaller than in the other cases. Similar conclusions can be made for the upper chord and for the other density profiles.

The slope of the Faraday rotation angle depends on both the central q value and the central density leading to the conclusion that the density profile should be measured in

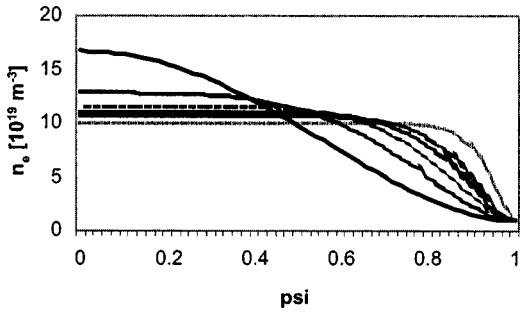

FIG. 6. Density profiles that have been used in the calculations. The profiles range from flat to peaked, but all have the same value of the line-averaged density.

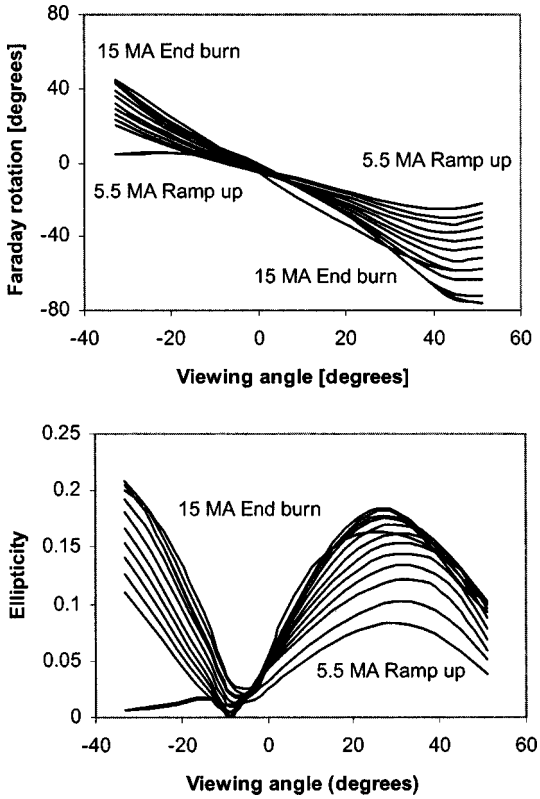

FIG. 7. Calculated Faraday rotation angles for a horizontal fan of chords (top) and the corresponding ellipticity values (bottom). The viewing angle is defined as the angle the chord makes with the equatorial plane (negative numbers refer to values below the midplane). The steepest slopes in the Faraday rotation correspond to the largest plasma currents. All values are for single passage of the beam.

conjunction with the Faraday rotation profile. This could be done either by interferometry along the same (polarimetry) chords (albeit that this method is very vulnerable to multiple fringe jumps and vibrations of the optical components, necessitating the use of a second wavelength) or by using the Cotton–Mouton effect to retrieve the electron density, as was originally proposed by Segre,[7] and already successfully demonstrated at W7-AS.[8] In this respect it should be mentioned that a polarimetric method proposed by Segre for ITER has been successfully tested at University College, Cork.[9] This method is based on a polarization modulation scheme that allows the simultaneous measurement of the Faraday rotation and the Cotton–Mouton effect by two, independent phase measurements, so that the diagnostic is virtually independent from intensity variations of the probing beam due to refraction and mechanical vibrations. In the test a sensitivity of about 1 deg with a time resolution of ~10 ms has been demonstrated. Complete polarimetry (i.e., the simultaneous measurements of the Faraday and the Cotton–Mouton effect) has been already successfully applied to the Joint European Torus plasma.[10]

The calculations presented in Fig. 6 and similar calculations for other cases demonstrate that physically speaking polarimetry at 118 μm is well feasible at ITER. However, they do not give an answer on the optimum number of chords of the polarimeter system. Therefore, it was decided to calculate the accuracy in the determination of the q profile

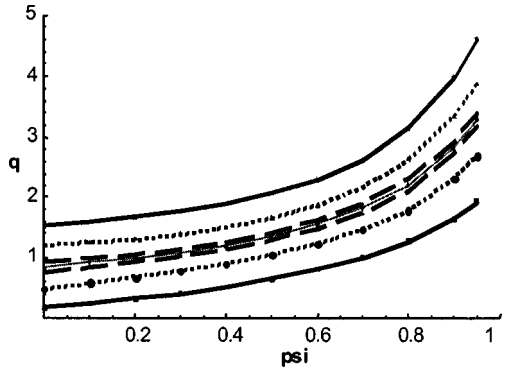

FIG. 8. Mean q profile, 95% database envelope (solid lines), 95% $2(\sigma)$ confidence bands for magnetics-only (dotted) and for magnetics +15 Faraday angles +15 line densities (dashed).

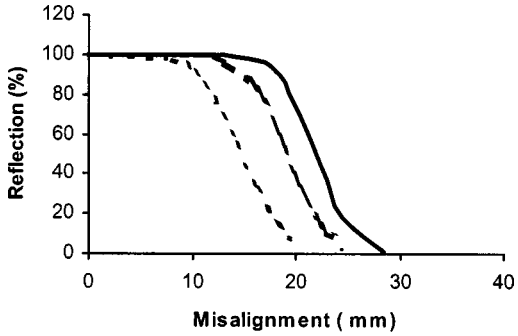

FIG. 10. Reflection of a Gaussian beam of 12 mm diameter vs the misalignment on the corner cube for three different retroreflectometer geometries. Solid: elongation oriented parallel to one interface: length: 60 mm, width: 37 mm; dashed: same as solid but for a length of 50 mm; dotted for a circular 37 mm diameter retroreflector.

using simulated polarimeter signals that were calculated from a database of in excess of 5000 lower single null equilibria (of which 1986 were selected for the present analysis). This database had been originally generated for the simulation of magnetic signals and has recently been extended by the computation of simulated polarimetry signals and the randomization of the plasma current. The equilibria were generated using a Database Generation and Analysis Package (DGAP). The core equilibrium calculation in DGAP is performed by the Garching equilibrium code. The database consists of $10<I_p<20$ MA, $B_0=5.3$ T lower X-point plasmas. The database contains a range of different q and density profiles.

Figure 8 shows the mean q profile generated from the database with the 95% (2σ) confidence bands using only the magnetic signals and using the magnetics plus 15 simulated Faraday rotation angles and 15 line densities. Noise was added to all simulated signals (15 mT on magnetics, 0.2° on Faraday rotation angles and 2×10^{17} m^{-3} on densities). Figure 9 shows the q-profile recovery error using only magnetic signals, magnetic + the equatorial polarimeter fan, and magnetics + both polarimeter fans.

The calculations shown in Figs. 8 and 9 have been done using the line density as measured by interferometry. However, an interferometer at ITER operating at 118 μm is expected to suffer from multiple fringe jumps. Therefore, it is planned to retrieve the electron density from the Cotton–Mouton effect measured along the same chord. The latter measurement is insensitive to fringe jumps and therefore much more robust. Simulations have been done using the density profile measured from the Cotton–Mouton effect instead of the interferometric density profile, leading to almost exactly the same conclusions with regard to the q-profile recovery error.

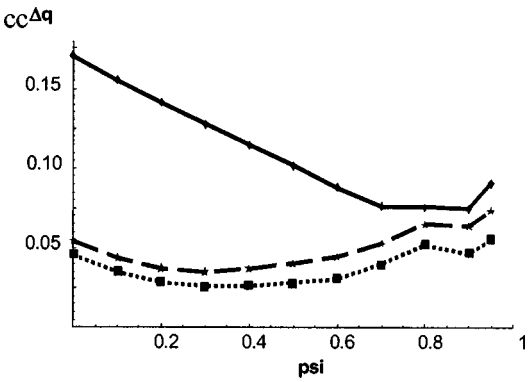

FIG. 9. Root mean square recovery error of the q profile (1σ here, 2σ in Fig. 7) vs the normalized poloidal flux for the magnetics-only base line model (solid), eight main plasma polarimetry chords (dashed), and all 15 chords (dotted).

It is clear from Figs. 8 and 9 that the data from the horizontal polarimeter fan give a substantial improvement of the q-profile determination in the plasma center. Including the chords via the upper port gives a further, but smaller, improvement. Analysis of the present database shows that the q-profile shapes can be described effectively with only six free parameters and, hence, may be artificially constrained thereby leading to an underestimation of the number of polarimeter chords necessary to adequately recover the profile.

IV. RETROREFLECTORS

As has been already stated in the introduction, the most critical elements of the polarimeter for ITER are the retroreflectors. To study the reflective properties of retroreflectors that are indented in a relatively deep (25 cm) slit, extensive ray-tracing calculations have been done.

In Fig. 10 the reflectivity is calculated for four different types of retroreflectors and as a function of the misalignment (in the poloidal direction) of the beam with respect to the center or the reflector. The conclusion is that it is advantageous to use a retroreflector that is elongated in a direction parallel to the slit in which it is placed. A 60 mm long, 37 mm wide retroreflector can cope with misalignments of up to 20 mm in the poloidal plane, without any effect on the reflectivity. This should give enough margin to cope with beam displacements due to refraction in the plasma. One of the interfaces of the elongated retroreflector should be oriented roughly vertical to minimize beam losses.

From Fig. 11 it is evident that it is important that the corners of the retroreflector are preferably sharper than 5% of the beam width for a >90% reflection. Although it is not difficult to manufacture retroreflectors with ideal sharp corners, care should be taken that the cumulative effects of ero-

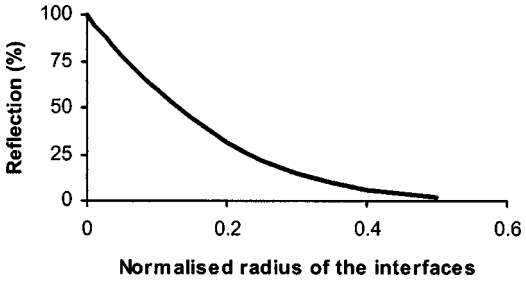

FIG. 11. Reflection of a centrally aligned Gaussian beam from a retroreflector as a function of the radius of curvature of the corners, normalized to the $1/e$ beam width.

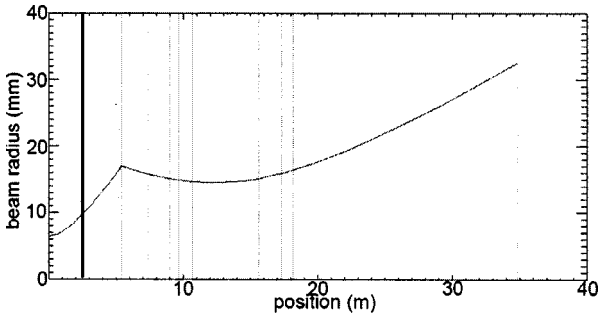

FIG. 12. Calculated waist (defined in terms of radius) of the full optical system from retroreflector up to the second focusing mirror, close to the entrance to the laser laboratory ($f_{\#3}=5100$ mm, $f_{\#12}=7200$ mm). The vertical lines show the locations of the optical components. The thick line refers to the position of the port penetration.

sion and deposition are small enough to not deteriorate the sharpness as a function of time. This implies that preferably materials with a low sputtering yield should be selected. Monocrystalline molybdenum seems to be the most promising material in this respect and is presently experimentally tested.

Apart from the fact that rounded corners have an effect on the absolute reflectivity, it also causes the reflectivity as a function of misalignment to become a nonmonotonic function with various local maxima and minima, which makes the alignment of the beam on the retroreflector (by searching for maximum reflection) much more difficult.

V. OPTICAL TRANSMISSION LINE

As was mentioned in Sec. II, the optical transmission from tokamak to diagnostics room will be a quasioptical system, evacuated up to the second vacuum window. The interspace between the two windows is separately pumped. The remainder of the oversized beam pipes is flushed with dry air or nitrogen to avoid absorption of the beam. The setup is rather similar to the polarimeter system that is used at the Reversed Field Experiment (RFX).[11] The latter system has a 31 m long transmission line flushed with dry nitrogen and features in total ten mirrors and mylar windows at either end. The transmission of this system amounts to 61%. Most of the attenuation of the beam is caused by the aluminium mirrors (their experimentally determined average reflectivity is 0.973 per mirror) and by the two mylar windows, which together have a transmission of 89%. Although the transmission system at ITER will be longer than that at RFX (about 44 instead of 31 m), it is obvious from the RFX experience that not the length of the transmission line, but the actual number of optical elements is decisive for the attenuation. Care should be taken to keep the number of mirrors as low as possible. The system at RFX will be used to investigate how the characteristics of key optical components such as the retroreflector and the beamsplitters that separate the incoming from the return beam can affect the measurements.

To get a feeling for the diameter of the beams along the optical system, and the required tolerances for the placement of optical components, as well as to study how the alignment of the beams can be maintained, Gaussian-beam ray-tracing calculations have been performed. A choice was made to do this for chord No. 5, which is the one that is probing just above the midplane (see Fig. 1). The coordinates of the various optical components are listed in Table I. The calculations were done from the retroreflector to the point of entrance in the diagnostic laboratory. The Gaussian-beam ray-tracing calculations have been performed with the computer program GRT3D, that was originally developed for the design of the interferometer system at the H-1NF heliac.[12]

As starting point of the calculations we defined the optimum beam waist at the position of the retroreflector to be 13 mm diameter (or as is further used in this article a beam radius of 6.5 mm). The calculated beam waist as a function of distance in the system is indicated in Fig. 12. The vertical lines indicate the positions of the various mirrors in the system. The vertical black line indicates the position of the port penetration. The following focal lengths have been used: $f_{\#3}=5100$ mm and $f_{\#12}=7200$ mm. The focal length of mirror No. 3 has been chosen such, that the beam radius in the optical system between mirror Nos. 11 and 12 is as small as possible. Also calculations have been done for other focal distances. A focal distance $f_{\#3}=4430$ mm (and $f_{\#12}=6731$ mm) results in the smallest beam diameter inside the port plug, which is advantageous because it leads to a lower neutron streaming. However, in case one also includes the necessity to have some extra margins in the diameter of the port penetrations to make it possible to align the beams one comes to the conclusion that the focal distances as used in Fig. 12 are the optimum ones. Figure 12 is reversible for the in- and outgoing beams as long as the beam is well aligned on the optical axis of the system.

Assuming an ideal alignment of the beam on the optical axis of the system, the minimum needed diameter of each optical element (as well as the diameter of beam penetrations) can be calculated. For the setup described here, this would imply that all optical elements from port penetration up to mirror No. 11 could be 75 mm diameter or less. However, as we shall see further, larger diameters will be needed to tolerate a certain degree of misalignment as well as to have the possibility to actively steer the beam for alignment purposes. Between mirror Nos. 11 and 12 the beam expands, but still fits in the 150 mm transmission pipes that are foreseen in the ITER design.

During operation of the polarimeter it can happen that due to any physical reason (e.g., refraction, movement of machine components), the beam is not well aligned onto the

retroreflector, or it may even miss the retroreflector completely. This can happen for one or more polarimeter chords simultaneously, while other chords maybe still well aligned. Therefore, it is proposed that as soon as the reflected signal for an individual chord becomes below a certain detection threshold, the chord is automatically switched from measuring mode to a scanning mode. In the latter mode, the beam is scanned over an area of 58×58 mm^2 at the position of the retroreflector. Because it is not easy to move any of the mirrors that are positioned close to the plasma (i.e., mirror Nos. 2 and 3) for obvious reasons, it is thought better to do the scanning by tilting a mirror that is further down the beam line. The best option seems to be to use mirror No. 5 for steering the beam. By tilting this mirror over ±0.32° in two directions, it is possible to scan the beam over an area of 58×58 mm^2 at the position of the retroreflector. The scanning will give rise to an additional displacement of the beam on the optical elements between the retroreflector and the scanning mirror (±20 mm at focusing mirror No. 3), which then defines the totally needed dimension of the beam penetration at each point as well as the needed dimensions of the various optical elements.

The transmission line from mirror No. 5 all the way to mirror No. 12 and even further into the diagnostic laboratory will be built as a fully articulated transmission line, which automatically keeps the alignment. With the GRT3D code we studied the maximum tolerable angular and transverse misalignments of the components in this beam line. The maximum tolerable angular misalignment is 10 mrad, and the maximum tolerable transverse misalignment is 1 mm (in a plane perpendicular to the beam axis) for all mirrors outside the bioshield. The effect of misalignments along the beam is very low and has not been considered. The earlier-mentioned tolerances are not extraordinary tough and it must be relatively straightforward to achieve them in a properly designed system.

VI. CALIBRATION

An important issue is to develop potential calibration strategies. However, it is very difficult to do this as long as the technical implementation of the polarimeter has not been fixed.[13,14] Nevertheless, it seems to be a rather obvious way to calibrate the polarimeter between consecutive ITER discharges. In that case, for an ideal optical system the expected Faraday rotation and Cotton–Mouton effect should be zero. However, coatings on especially the first and second mirror, nonideal behavior of the retroreflector, and birefringence in windows can lead to a nonzero rotation of the plane of polarization of the beam as well as to a nonzero ellipticity. The cumulative effect of these can be measured in absence of the plasma and then corrected for during plasma operation.

It would good if also a provision is added to quantitatively induce a polarization in the beam (in case of no plasma). In many present polarimeters rotating polarizers are used to quantitatively calibrate the system. Since in the ITER polarimeter the beam returns along the same path, it is not possible to use rotating semireflective plates for purpose. Instead one should employ rotating polarizer grids that can be moved in to/out off the beams.

VII. OUTLOOK

As was stated in the introduction, polarimetry is not the only method that can measure the current density profile. Therefore it is important to extend the simulation studies reported in Sec. III, to find the optimum combination of magnetics, polarimetry chords, and MSE observation chords to retrieve the q profile in ITER within the requirements set by the ITER team.

Additionally detailed testing of prototype retroreflectors is underway. This is at the one hand done by exposing the retroreflectors to bombardment with deuterium ions from a source, after which the reflectivity and the polarization characteristics are measured at 118 μm. On the other hand, prototype retroreflectors are exposed to the Tore Supra plasma to get an idea of their vulnerability to erosion and deposition as a function of time. Furthermore, it was shown in literature that the polarization state of the retroreflected beam may depend on the specific region of the retroreflector hit by the incoming beam.[15,16] The polarization is only preserved when the retroreflector is illuminated in such a way that all the radiation in the beam cross section undergoes the same sequence of three reflections. As this is difficult to achieve in the ITER design (a very small beam waist at the retroreflector would be required), it can be expected that movements of the beam within the 37 mm diameter active area of the corner cube, would introduce changes of the polarization status that are in principle indistinguishable from those due to the plasma. The importance of this effect needs to be investigated experimentally.

A further important aspect that has not yet been addressed in our study is the effect the various optical components (mirrors, windows, beam splitters, etc.) have on the polarization of the beam. It is obvious that the various optical elements (including possible deposition layers) should cause a minimum distortion to the polarization ellipse of the beam. This, however, is strongly related to the polarimetry scheme that is adopted for ITER. Therefore, the various schemes (based on static, rocking, and rotating linearly polarized input beams, counterpropagating circularly polarized beams, etc.) should be studied in detail to assess their possible merit for ITER. It is foreseen that many of these aspects can be tested in the mock up that is available at the RFX experiment in Padova (see Sec. V).

ACKNOWLEDGMENTS

The authors would like to thank George Warr and John Howard of the Australian National University for providing the GRT3D Gaussian ray-tracing code. This work, supported by the European Communities under the contract of Association between EURATOM/FOM, was carried out within the framework of the European Fusion Development Agreement.

[1] F. DeMarco and S. E. Segre, Plasma Phys. **14**, 245 (1972).
[2] A. Boileau *et al.*, J. Phys. B **22**, L145 (1989); F. M. Levinton *et al.*, Phys. Rev. Lett. **63**, 2060 (1989).

[3] A. J. H. Donné *et al.*, Rev. Sci. Instrum. **70**, 726 (1999).
[4] D. Véron, in *Infrared and Millimeter Waves*, edited by K. J. Button (Academic, New York, 1979), Vol. 2.
[5] D. Elbeze *et al.*, Rev. Sci. Instrum. **75**, 3405 (2004).
[6] C. Nieswand, in *Diagnostics for Experimental Thermonuclear Fusion Reactors 2*, edited by P. E. Stott *et al.* (Plenum, New York, 1998), pp. 213–216.
[7] S. E. Segre, Phys. Plasmas **2**, 2908 (1995).
[8] Ch. Fuchs and H. J. Hartfuss, Rev. Sci. Instrum. **70**, 722 (1999).
[9] L. Giudicotti *et al.*, Plasma Phys. Controlled Fusion **46**, 681 (2004).
[10] K. Guenther *et al.*, Reported at the 4th Meeting of the ITPA Topical Group on Diagnostics, Padua, 2003.
[11] E. Zilli *et al.*, Int. J. Infrared Millim. Waves **21**, 1673 (2000).
[12] G. B. Warr and J. Howard, Rev. Sci. Instrum. **72**, 2305 (2001).
[13] J. H. Rommers *et al.*, Plasma Phys. Controlled Fusion **40**, 2073 (1998).
[14] A. J. H. Donné, Rev. Sci. Instrum. **66**, 3407 (1995).
[15] S. E. Segre and V. Zanza, J. Opt. Soc. Am. A **20**, 1804 (2003).
[16] C. Gil, work published under an EFDA contract (not publicly available).